

Immunofluorescence confocal laser scanning microscopy and immuno-electron microscopic identification of keratins in human materno-foetal interaction zone

J. Ahenkorah^a, B. Hottor^a, S. Byrne^a, P. Bosio^b, C. D. Ockleford^{a, c, *}

^a *Laboratory for Developmental Cell Sciences, Department of Infection Immunity and Inflammation, School of Medicine and Biological Sciences, University of Leicester Medical School, Leicester, UK*

^b *Department of Cancer Studies, Molecular Medicine and Reproductive Science, University of Leicester, Leicester Royal Infirmary, Leicester, UK*

^c *Department of Medicine, Lancaster University, Lancaster, UK*

Received: January 16, 2008; Accepted: April 21, 2008

Abstract

We show here that at least 5 keratin proteins are present in villous trophoblast and the same 5 in extravillous trophoblast. A further 14 tested were undetectable in these tissues. In contrast, 10 of the 19 keratins tested were present in amniotic epithelium. The marking of amniotic epithelium on the one hand, as distinct from villous and extravillous trophoblast on the other, can be achieved using 5 keratins (K4, 6, 13, 14 and 17) with a mixture of positive and negative discrimination that is expected, in combination, to be highly sensitive. All the specific keratins identified in trophoblast were apparently up-regulated on the pathway to extravillous trophoblast. Co-ordinated differentiation at the molecular expression level is indicated by this finding. The relevant keratins are K5, 7, 8, 18 and 19. Specific keratins have been identified that are down-regulated in villous trophoblast in pre-eclamptic pregnancy. This difference between healthy and pre-eclamptic chorionic villous trophoblast keratin expression was statistically significant in 4 out of the 5 keratins. This was not the case for the extravillous trophoblast at the immunofluorescence confocal level but significant differences were obtained using immunogold electron microscopy. We suggest that the villous trophoblast in pre-eclamptic placentae is cytoskeletally weaker with respect to the filaments made from these specific proteins and that this is one reason why, in pre-eclampsia, trophoblast is deported in greater quantity than in healthy placentae.

Keywords: keratin immunofluorescence • materno-foetal interaction • chorionic villi • pre-eclampsia

Introduction

Trophoblast is a family of ectodermal epithelial tissues that constitute the outer envelope of the conceptus [1]. Its cells and syncytia perform several key roles in implantation, placentation, pregnancy maintenance and parturition [2, 3]. It is also of significance in pregnancy pathologies [4, 5]. A characteristic cytoskeletal marker of extra-embryonic membrane epithelia is the 10 nm diameter bundles of intermediate filaments comprised of keratins [6–8]. Cytokeratins now called Keratins (Ks) according to the new nomenclature system [9] are known to be the major structural proteins of epithelial cells, which help maintain their structural

integrity. They are grouped into two types. Type II keratins are a family of basic proteins identified as K1 to K8, whereas type I keratins that consist of K9 to K20, belong to the acidic group [10]. Most keratins genes are regulated in a pair wise, tissue and differentiation-specific manner and have been used as a tool in the study of epithelial tissues in health and disease [11]. The heteropolymeric interaction of pairs of keratins in filament formation means that more than one keratin protein is always found in these cells. In the natural world, we know of a very large number of keratin proteins including those of epithelia such as skin and skin derivatives such as hair, some horns and feathers. Genomic analysis has shown that human beings possess a total of 54 functional keratin genes (28 type I and 26 type II) located on chromosomes 17 and 12 [12–15]. More than 30 keratins and tricycote keratins (hard or hair/nail keratins) [16] have been described in the human body and these are potential markers of differentiation of ectodermal cell lineages and pathological change [4, 5, 17–21]. The human placental

*Correspondence to: C. D. OCKLEFORD,
Department of Medicine, Faraday Building,
Lancaster University, Lancaster LA1 4YB, UK.
Tel.: +44(0) 1524 594515
Fax: +44(0) 1524 593747
E-mail: C.Ockleford@lancaster.ac.uk

trophoblast is reported to express keratins in developmental-, differentiative- and functional-specific patterns [22]. It is known that simple epithelia express K8/K18 with variable levels of K19 and K20, whereas stratified epithelia like the skin express K5/K14 basally and K1/K19 suprabasally [23]. For this reason, we have undertaken the most comprehensive analysis to date of the trophoblastic keratins that can be identified using a panel of specific antibodies.

The chorion is the superficial layer of the conceptus. Its name is derived from a word literally meaning skin and can therefore be viewed as a form of capsule that has major interfaces with maternal blood (the chorionic villous trophoblast: CVT) and the maternal decidua tissues (basal plate extra-villous trophoblast: EVT and chorion laeve trophoblast CLT). Essential differences between the two forms of trophoblast include that the latter has been responsible for invasive, motile and attachment functions whilst the former has transport, endocrine and other functions. The villous trophoblast is believed to be the source of deported trophoblast that is shed extensively into the maternal blood [24]. The reduction in keratin expression in chorionic villous trophoblast that occurs in pre-eclampsia is significant [4, 5]. Earlier we proposed that as a result of this phenomenon the villous trophoblast syncytioskeleton would be expected to become mechanically less strong, so promoting the observed increase in the deportation of trophoblast towards term in pre-eclamptic pregnancy. In this paper, we identify the specific molecules concerned.

Materials and methods

Ethics and patient recruitment

Approval for the study was obtained from the Leicestershire Research Ethical Committee Ref 7144, and the University Hospitals of Leicester NHS Trust Research and Development Committee Ref UHL9161. At the Pregnancy Hypertension Unit of the Leicester Royal Infirmary (LRI), suitable candidates for the study were identified during admission to the ward. The classification criteria used for diagnosis of pre-eclampsia was based on those published by the American College of Obstetrics and Gynaecology (ACOG practical bulletin) [25] and consistent with the consensus from the international society for the study of hypertension in pregnancy (ISSHP). The criteria for selection included: clinical diagnosis of pre-eclampsia supported by laboratory investigations, Caucasian race and nulliparity. Multiparity, multiple pregnancies and women with medical conditions such as hypertension and diabetes were excluded from the study. Informed consent, in writing, was obtained from suitable candidates. These candidates were then monitored until they delivered, either normally or by caesarean section, placental basal plate samples were collected within 1 hr of delivery.

Tissue collection and sampling method

A total of 20 placental samples (n) were collected. This included 10 normal pregnancy placentae and 10 pre-eclamptic pregnancy placentae. Four (1 cm × 1 cm × 0.5 cm) blocks were sampled per basal plate.

Freeze-fixation

The samples were placed on ice in a Dewar flask for transport and immersed in OCT embedding medium (Tissue-Tek, Sakura Finetek Europe) in aluminium foil moulds and then freeze-fixed in a liquid hexane and dry ice slush. Frozen specimens were stored in a -80°C freezer.

Cryosectioning

7- μm -thick sections were cut using a Bright cryo-microtome and thawed on 'subbed' Super Frost slides. The sections were fixed in 1:1 Acetone-methanol at room temperature for between 5 and 10 min. After fixation, slides were washed 5 times 5 min. in 20 mM Tris buffered saline pH 7.6 with 0.1% Tween-20 (TBS-T).

Antibodies

Initial experiments used a mouse monoclonal anti-pan-cytokeratin-IgG₁ isotype as a trophoblast marker, which is a 'cocktail' of K4, 5, 6, 8, 10, 13 and 18 (Sigma-Aldrich, MO, USA, C2931) [5]. This was diluted in TBS-T containing 20% foetal calf serum, 1:800. The secondary antibody for the trophoblast marker was Cy3-conjugated sheep antimouse Affinipure IgG Fab₂ (Jackson ImmunoResearch Laboratories, West Grove, PA, USA, 51787) at a dilution of 1:1200.

All primary antibodies in the present study were monoclonal, raised in mouse, except K3 and K12, which were goat polyclonal antibodies. The secondary antibodies were FITC-conjugated sheep antimouse IgG (Sigma-Aldrich F-3008 Lot 128H9153) and FITC-conjugated rabbit anti-goat IgG (Sigma-Aldrich product No.F-2016). These antibodies were diluted in TBS-T containing 20% foetal calf serum as shown in Table 1. Optimum dilutions were ascertained by titration.

Slide mounting

After washing in TBS-T, slides were blotted. Sections on the slides were outlined using a slide marker pen that formed a hydrophobic ring that retained the antibodies applied to the tissue. The section was then flooded with 100 μl of the diluted primary antibody preparation and incubated at 4°C overnight in a humid atmosphere.

Following an overnight incubation, slides were washed, 5 × 5 min., in 20mM Tris Buffered Saline with 0.1% Tween-20 (TBS-T). Subsequently, 100 μl of secondary antibodies were applied to the tissue and the slides were incubated for 1–2 hrs at room temperature in a dark cabinet.

Slides were then washed 5 × 5 min. in (TBS-T), then the slides were covered with glass coverslips using an aqueous mountant Mowiol 4-88 from Calbiochem containing the anti-photobleaching agent DABCO (Diazabicyclo [2.2.2] octane).

Control experiments

Control experiments were carried out by omission of the primary antibodies and their replacement by 20% foetal calf serum or an isotype control antibody applied at the same dilution as the primary antibody.

Table 1 Properties of the antibodies used for immunocytochemical and immuno-electron microscopic localisation of keratins described in the text.

Anti-keratin	Source	Clone	Primary dilution	Secondary dilution	Isotype
K1	Santa Cruz Biotechnology, Inc.	LHK1,# sc-53249	1:50	1:100	IgG _{2a}
K2	Santa Cruz Biotechnology, Inc.	AE3,# sc-57004	1:20	1:100	IgG ₁
K3	Santa Cruz Biotechnology, Inc.	Q-14,# sc-49181	1:50	1: 100	IgG
K4	Sigma-Aldrich	6B10,# C5176	1: 20	1:50	IgG ₁
K5	Santa Cruz Biotechnology, Inc.	RCK103,# sc-32721	1: 50	1: 100	IgG ₁
K6	Serotec	LHK6B, MCA 1869	1: 20	1: 50	IgG _{2a}
K7	Sigma-Aldrich	LDS-68,#C6417	1: 150	1: 50	IgG ₁
K8	Sigma-Aldrich	M20,#C5301	1: 400	1: 50	IgG ₁
K9	American Research products, Inc. TM	Ks 9.70 & Ks 9.216	1: 20	1: 100	IgG ₁ + IgG ₃
K10	Serotec	MCA 1871T, #070905	1: 40	1: 50	IgG ₁
K12	Santa Cruz Biotechnology, Inc.	L-20,sc-17099	1: 50	1: 100	IgG
K13	Sigma-Aldrich	KS-1A3,#C0791	1: 20	1: 50	IgG ₁
K14	Sigma-Aldrich	CKB1,#C8791	1: 50	1: 50	IgM
K15	Santa Cruz Biotechnology, Inc.	LHK15, sc-47697	1: 50	1: 100	IgG
K16	Santa Cruz Biotechnology, Inc.	LL025, sc-53255	1: 50	1: 100	IgG
K17	Sigma-Aldrich	CK-E3,#C9179	1: 50	1: 50	IgG _{2b}
K18	Sigma-Aldrich	CY-90,#F4772	1: 1000	1: 60	IgG ₁
K19	Sigma-Aldrich	A53-B/A2	1: 50	1: 60	IgG _{2a}
K20	Santa Cruz Biotechnology, Inc.	Q2,#8c-58730	1: 20	1: 100	IgG ₁

Suppliers details are as follows Santa Cruz Biotechnology Inc., Santa Cruz, CA, USA; Sigma-Aldrich, St. Louis, MO USA; AbD Serotec, MorphoSys UK Ltd., Kidlington, Oxford, UK; American Research Products, IncTM ARP, Belmont, MA, USA.

Epifluorescence microscopy

A Zeiss epifluorescence microscope fitted with filter sets for Cy-3 and FITC fluorophores was used to pre-screen samples. Well-labelled sections were selected for confocal laser scanning microscopy.

Confocal laser scanning microscopy (CLSM)

Tissue sections were viewed using a Biorad MRC 600 CLSM attached to a Zeiss Axiovert inverted microscope. With the laser source set at zero, gain at 8 for the green channel, objective lens magnification

Table 2 K7 statistics

Tissue	<i>n</i>	Min	Max	% Median pixel value	25 th percentile	75 th percentile
CVTp	95	0.00	4.10	0.04	0.00	0.18
EVTp	95	0.03	15.94	2.93	1.36	6.08
CVTh	95	0.00	5.60	0.17	0.02	0.75
EVTh	95	0.01	17.97	4.06	1.76	7.07

The table shows the results of statistical analysis of the keratin 7 (K7) immunofluorescence intensity data in pre-eclamptic chorionic villous trophoblast (CVTp) pre-eclamptic extravillous trophoblast (EVTp) and their healthy control tissues (CVTh and EVTh). The statistically significant level was set at *P* less than 0.05 for data in tables 2–5: outcomes were assigned as follows:-

Wilcoxon sign-rank test:

Comparing CVTp and EVTp [$Z = -8.463, P = 0.0001$]***

Comparing CVTh and EVTh [$Z = -8.248, P = 0.0001$]***

Two sample Wilcoxon rank-sum (Mann-Whitney) Test:

Comparing CVTp and CVTh [$Z = -3.262, P = 0.0011$]***

Comparing EVTp and EVTh [$Z = -1.509, P = 0.1312$] ns

Table 3 K8 statistics

Tissue	<i>n</i>	Min	Max	% Median pixel value	25 th percentile	75 th percentile
CVTp	89	0.00	7.22	0.03	0.00	0.20
EVTp	89	0.60	11.40	1.86	1.13	3.55
CVTh	89	0.00	8.96	0.32	0.03	0.88
EVTh	89	0.17	13.75	2.88	1.00	4.86

The table shows the results of statistical analysis of the keratin 8 (K8) immunofluorescence intensity data in pre-eclamptic chorionic villous trophoblast (CVTp) pre-eclamptic extravillous trophoblast (EVTp) and their healthy control tissues (CVTh and EVTh). Significance was assigned as follows:-

Wilcoxon sign-rank test:

Comparing CVTp and EVTp [$Z = -7.974, P = 0.0001$]***

Comparing CVTh and EVTh [$Z = -7.624, P = 0.0001$]***

Two sample Wilcoxon rank-sum (Mann-Whitney) Test:

Comparing CVTp and CVTh [$Z = -3.342, P = 0.0008$]***

Comparing EVTp and EVTh [$Z = -1.751, P = 0.0799$] ns

was $\times 20$. Tissue was scanned with minimum pixel dwell time to limit photobleaching.

Measurement

Using COMOS software, images of anti-keratin immunofluorescence were obtained for healthy and pre-eclamptic placentae, comprising both chorionic villous trophoblast (CVT) and extravillous trophoblast (EVT) of the basal plate tissue. Images were measured using the same rectangular boxed area of $340.80 \times 226.60 \mu\text{m}$ ($77,225.28 \mu\text{m}^2$). Percentage of pixels with intensity in the high intensity (Band 210–255) for both (CVT) and (EVT) were recorded. The criteria for taking measurements were to randomly select regions of EVTs or CVTs on the same basal plate tissue image and to ensure that each area selected to be measured did not overlap an area already cho-

sen. Paired measurements of areas of EVT and CVT in each image from the same section were made. This was done to minimize the effects on the comparison of inter-preparation variation. The area to be measured contained only either EVT or CVT. Results were recorded in Excel spreadsheets and statistical analyses were carried out using STATA™ version 9.2 (StataCorp, College Station, TX, USA). The *n* values listed in Tables 2–5 and used for Figs 4–7 were the number of boxed areas scanned. Where quantitative data are presented all the antibodies were applied to the same range of tissues.

Tissue samples and fixation for transmission electron microscopy (TEM)

Four placentae were obtained from the Maternity Unit at Leicester Royal Infirmary, two following normal, uncomplicated births and two from

Table 4 K18 statistics

Tissue	<i>n</i>	Min	Max	% Median pixel value	25 th percentile	75 th percentile
CVTp	85	0.00	2.44	0.08	0.01	0.23
EVTp	85	0.00	11.66	2.11	1.00	4.12
CVTh	85	0.00	7.18	0.50	0.18	1.05
EVTh	85	0.11	14.66	2.90	1.54	4.70

The table shows the results of statistical analysis of the keratin 18 (K18) immunofluorescence intensity data in pre-eclamptic chorionic villous trophoblast (CVTp) pre-eclamptic extravillous trophoblast (EVTp) and their healthy control tissues (CVTh and EVTh). Significance was assigned as follows:-

Wilcoxon sign-rank test:

Comparing CVTp and EVTp [$Z = -7.905, P = 0.0001$]***

Comparing CVTh and EVTh [$Z = -7.328, P = 0.0001$]***

Two sample Wilcoxon rank-sum (Mann-Whitney) Test:

Comparing CVTp and CVTh [$Z = -6.117, P = 0.0001$]***

Comparing EVTp and EVTh [$Z = -1.789, P = 0.0736$] ns

Table 5 K19 statistics

Tissue	<i>n</i>	Min	Max	% Median pixel value	25 th percentile	75 th percentile
CVTp	83	0	1.97	0.01	0.00	0.06
EVTp	83	0	9.26	0.62	0.21	1.77
CVTh	83	0	1.38	0.04	0.00	0.10
EVTh	83	0	9.50	1.06	0.42	2.45

The table shows the results of statistical analysis of the keratin 19 (K19) immunofluorescence intensity data in pre-eclamptic chorionic villous trophoblast (CVTp) pre-eclamptic extravillous trophoblast (EVTp) and their healthy control tissues (CVTh and EVTh). Significance was assigned as follows:-

Wilcoxon sign-rank test:

Comparing CVTp and EVTp [$Z = -7.478, P = 0.0001$]*** up-regulated

Comparing CVTh and EVTh [$Z = -7.693, P = 0.0001$]***

Two sample Wilcoxon rank-sum (Mann-Whitney) test:

Comparing CVTp and CVTh [$Z = -1.941, P = 0.0522$] * threshold

Comparing EVTp and EVTh [$Z = -1.867, P = 0.0619$] ns

pre-eclamptic pregnancies. Informed consent was obtained according to local ethical committee guidelines (as above). Small pieces of basal plate ($10 \times 10 \times 2$ mm) were excised within minutes of delivery and fixed for 1 hr in 4% paraformaldehyde, 0.1% glutaraldehyde in phosphate-buffered saline (PBS), dehydrated through an ethanol series and embedded in LR White (London Resin Company, Reading, Berkshire, UK).

Thin sectioning and TEM Immuno-labelling

Semi-thin (0.5–1.0 μ m) sections were baked onto glass slides, stained with 1% toluidine blue and viewed microscopically. Favourable regions of these sections were chosen, so that the large block face could be trimmed down to a size suitable for ultramicrotomy. Thin (80–100 nm) sections

from these were collected on 200-mesh nickel grids. When the sections were dry, they were 'blocked' against non-specific antibody binding by flotation on droplets of 2% normal goat serum (NGS) / 1% bovine serum albumin (BSA) / 1% Tween-20 in phosphate-buffered saline (PBS-T) for an hour at room temperature. The experimental primary antibodies were anti-keratin 18 and anti-keratin 7 (clone number CY-90: product number C8541; Sigma for K18 and clone number LDS-68: product number C6417 for K7).

For K18, the grids after blocking were floated on 10 μ l droplets of the primary antibody solution 1:100 at 4°C overnight. After overnight incubation, the grids were given 6×5 min. washes in PBS-T, then transferred onto blocking solution and finally, the sections were incubated in a 1:50 dilution of goat antimouse IgG whole molecule conjugated to 10 nm gold particles (product number G7777 lot 084k1581, Sigma) at room temperature.

With the keratin 7 antibody, grids were first placed in a cassette and immersed in an epitope unmasking solution of 10 mM citrate buffer, pH 6.0 for 20 min. at 95°C. The grids with the cassette were removed gently and allowed to cool down in cold citrate buffer for 20 min. The grids were then dipped 10 times in two changes of distilled water before floating on 'blocking solution' and then transferred onto 10 μ l droplets of the antibody with a working dilution of 1:20 in blocking solution and incubated at 4°C overnight. After overnight incubation and washing as above, the sections were incubated in a 1:50 dilution of goat antimouse IgG whole molecule conjugated to 10 nm gold particles at room temperature.

Negative control experiments were carried out without the primary antibodies and these confirmed the specificity of the labelling procedure.

Slides were thoroughly washed first in PBS-T, then in distilled water. They were then air dried and the sections were stained in 5% uranyl acetate in 9% aqueous isobutanol, washed again in distilled water, air-dried and viewed using a JEOL JEM-1220 transmission electron microscope at 10,000–40,000 \times magnification.

Counting of gold particles

Areas that included obvious intermediate filament bundles were circumscribed and the numbers of gold particles within these areas were counted. Areas on the electron micrographs containing the nucleus were also circumscribed and any gold particles counted were recorded as background. Counts were made for images from CVT and EVT for healthy and pre-eclamptic placentae. A 1- μ m² area (from the scale bar on the print) was cut out of the paper and weighed using a 1-mg balance. The circumscribed areas were similarly cut out and weighed; the counts associated with these were recorded and this allowed the number of gold particles per μ m² to be calculated for each area and cell type. All micrographs counted were taken at the same magnification \times 40,000.

Results

The CLSM images (Figs 1–3) reveal specific anti-keratins indirect immunofluorescence labelling of the cytoplasm of trophoblast.

An interesting feature of the anti-keratin immunofluorescence micrographs of basal plate is that the extra-villous trophoblast cells, which stand out clearly, are unevenly distributed. Clusters of relatively high EVT density are interspersed with regions of low density. This can be contrasted with the situation in chorion leave where there is a relatively even and continuous layer that is 5–7 cells thick. The origin of extravillous trophoblast is thought to be from the cytotrophoblast cell columns of the anchoring villi. It is thus probable that initially their distribution is uneven over the basal plate and highest at their points of contact with anchoring villi (the source) and lowest at the furthest points from the anchoring villous attachment. In a few instances, cells of the EVT occur in linear alignment (Fig. 1E). These are clearly not complete epithelial sheets similar to the amniotic epithelium but are an interesting epithelium-like feature.

The degree of difference in immunofluorescence intensity can be highlighted by a banding procedure (Figs 2 and 3, left panels),

where a threshold of immunofluorescence intensity is set and all pixels in the image above that level of intensity are colour-coded (here in red). A plot of the incidence of high-intensity pixels in the range 210–255 comparing areas of the image occupied by EVT (blue) and CVT (pink) shows a consistent excess of high greyscale value pixels in the EVT areas. The pattern of expression of specific keratin immunofluorescence is described in Figs 4–7 and the statistical analysis is shown in Tables 2–5. The overall picture is summarised in Table 6.

We have demonstrated that keratins 5, 7, 8, 18 and 19 are found in both villous and extravillous trophoblast and that at least 4 out of the 5 keratins are up-regulated on the differentiation pathway from villous to extravillous trophoblast in a highly statistically significant manner (Tables 2–6). The up-regulation in K5 (Fig. 1H) was observed as it followed the same pattern as the others. Keratins 1, 2, 3, 4, 6, 9, 10, 12, 13, 14, 15, 16, 17 and 20 are not detectable in villous and extravillous trophoblast. All of the keratins tested were found in amniotic epithelium with the definite exception of keratin 1, 2, 3, 7, 9, 12, 15, 16 and 20 (Table 6).

Statistical analysis

The statistical analysis of the data is summarized here on a keratin by keratin basis. The analysis reveals the significance levels between the random samples from the different tissues in healthy and pre-eclamptic placentae (Figs 4–7).

K7

Comparing CVTp and CVTh,

$z = -3.262$ and the probability $p|z| = 0.0011^{***}$

Comparing EVTp and EVTh,

$z = -1.509$ and the probability $p|z| = 0.5368$ ns

K8

Comparing CVTp and CVTh,

$z = -3.342$ and the probability $p|z| = 0.0008^{***}$

Comparing EVTp and EVTh,

$z = -1.751$ and the probability $p|z| = 0.0799$ ns

K18

Comparing CVTp and CVTh,

$z = -6.117$ and the probability $p|z| = 0.0001^{***}$

Comparing EVTp and EVTh,

$z = -1.789$ and the probability $p|z| = 0.4566$ ns

K19

Comparing CVTp and CVTh,

$z = -1.941$ and the probability $p|z| = 0.0522^{**}$

Comparing EVTp and EVTh,

$z = -1.867$ and the probability $p|z| = 0.0619$ ns

Immuno-electron microscopy

Electron micrographs of trophoblast anti-keratin immuno-gold labelling show clearly that this is predominantly overlying bundles of intermediate filaments. It does not occur over the nuclei,

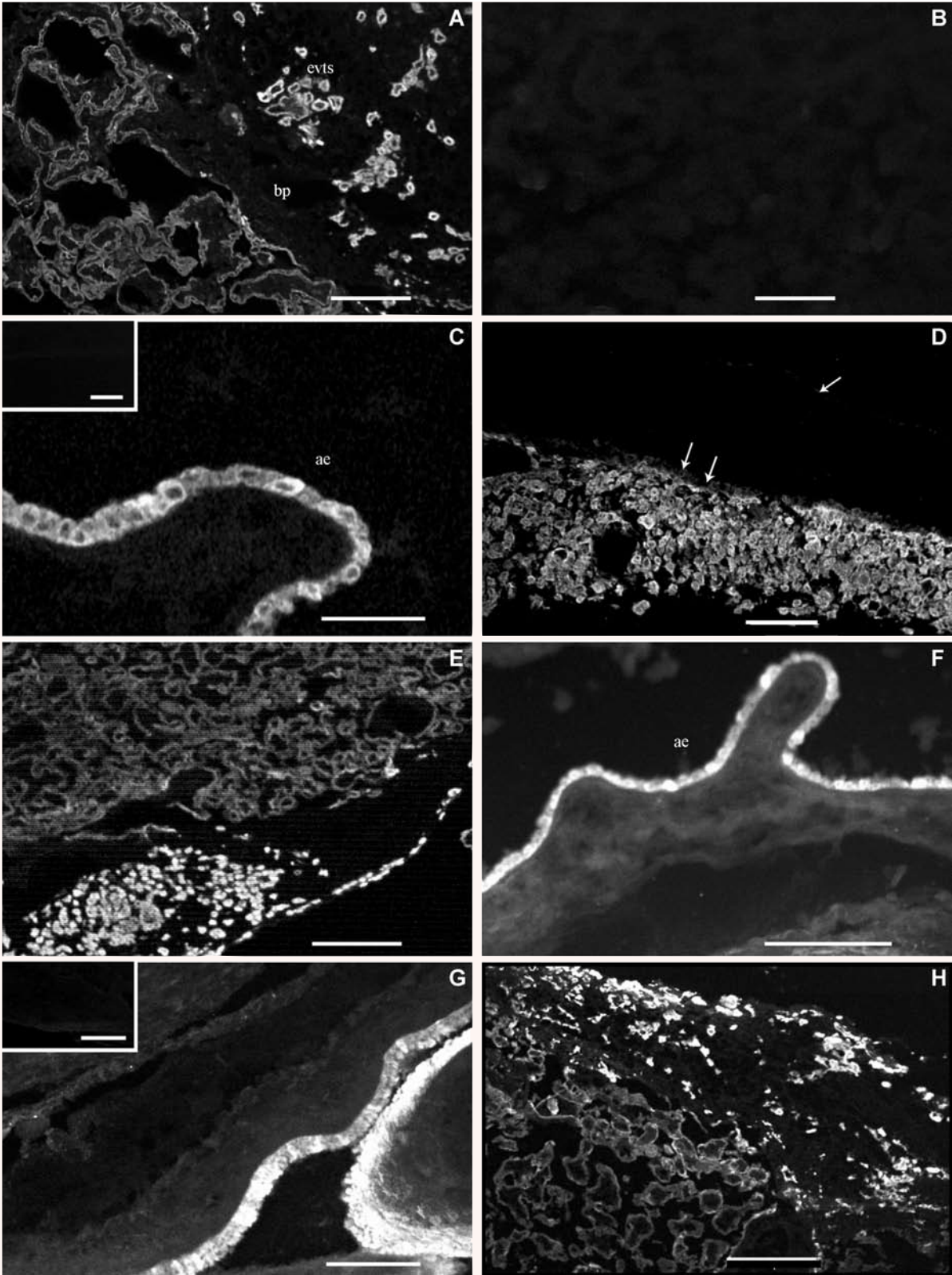




Fig. 1 (A) Keratin 7 distribution over the villous tree (lower left) separated by the basal plate (bp) from extravillous trophoblast (evts: upper right). The immunofluorescence intensity is positive over the villous epithelium and the extravillous trophoblast cells, but much more intense over the latter. Scale bar = 250 μ m. (B) Isotype control with mouse IgG₁ same dilution of 1:150 as anti-K7 antibody. Scale bar = 250 μ m. (C) Anti-keratin 17 immunofluorescence distribution over the amniochorion. The immunofluorescence is intense over the amniotic epithelium cytoplasm. Note that the compact, fibroblast, spongy and reticular layers and the chorion leave trophoblast cells are unlabelled. Scale bar = 25 μ m. Inset: Anti-keratin 17 distribution over a region containing villous and extravillous trophoblast. The immunofluorescence intensity is below the background level of detection. Scale bar = 100 μ m. (D) Anti-keratin 7 immunofluorescence of amniochorion. Note that the amniotic epithelium (single arrow) is scarcely above background levels whilst the EVT's in the chorion (double arrows) are highly immunoreactive. Scale bar = 250 μ m. (E) Immunofluorescence of anti-keratin 7 showing a cluster of brightly immunofluorescent EVT's and linear stretch of EVT's (lower right) in the basal plate tissue. As usual the chorionic villi are less immunoreactive. Scale bar = 250 μ m. (F) Anti-keratin 13 immunofluorescence of amniochorion. Scale bar = 100 μ m. (G) Anti-keratin 14 immunofluorescence of amniotic epithelium. Scale bar = 25 μ m. Inset: Basal plate tissue showing no immunofluorescence above background. Scale bar = 100 μ m. (H) Anti-keratin 5 immunofluorescence of basal plate tissue. It is of low intensity on the lower part (CVT's) and brighter on the upper part (EVT's). Scale bar = 250 μ m.

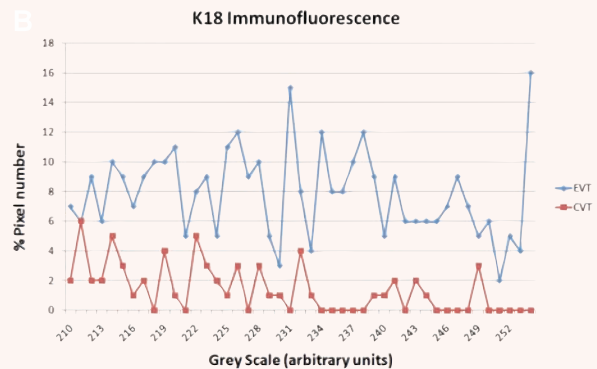
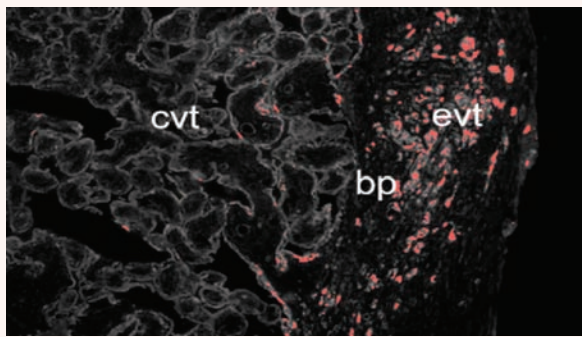


Fig. 2 (A & B) The graph on the right shows the pixel intensity distribution over areas of chorionic villous trophoblast (pink line) and extravillous trophoblast (blue line) when indirect immunofluorescence preparations of keratin 18 are imaged. The areas sampled for the intensity distribution graphs are shown on the left and the pixels of highest greyscale value (210–255) equivalent to immunofluorescence intensity have been banded red. The red banding corresponds to the location of EVT and is only infrequently seen in chorionic villous trophoblast.

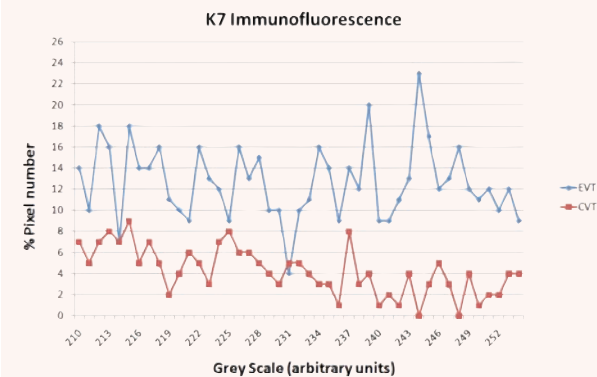
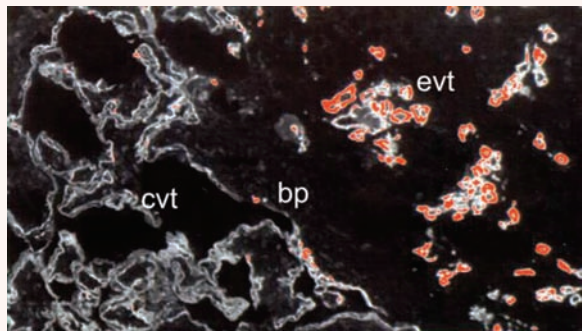


Fig. 3 (A & B) This is an indirect immunofluorescence preparation using anti-keratin 7. The areas sampled for the intensity distribution graphs are shown on the left and the pixels of highest grey scale value (210–255) equivalent to immunofluorescence intensity have been banded red. The red banding corresponds to the location of EVT and is only infrequently seen in chorionic villous trophoblast. The graph on the right shows the pixel intensity distribution of high greyscale pixels within this brightness band over areas of chorionic villous trophoblast (pink line) and extravillous trophoblast (blue line).

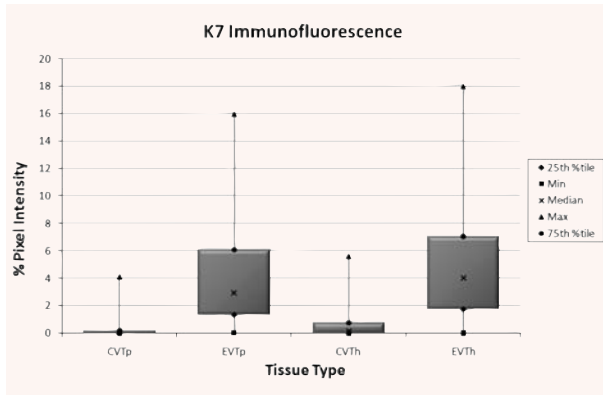


Fig. 4 Boxplot showing interquartile range of the CLSM immunofluorescence data using the anti-keratin-7 antibody on pre-eclamptic chorionic villous trophoblast (CVTp) and extravillous trophoblast (EVTp), also healthy chorionic villous trophoblast (CVTh) and extravillous trophoblast (EVTh). The minimum, median and maximum values are indicated by the key and the whisker shows the range.

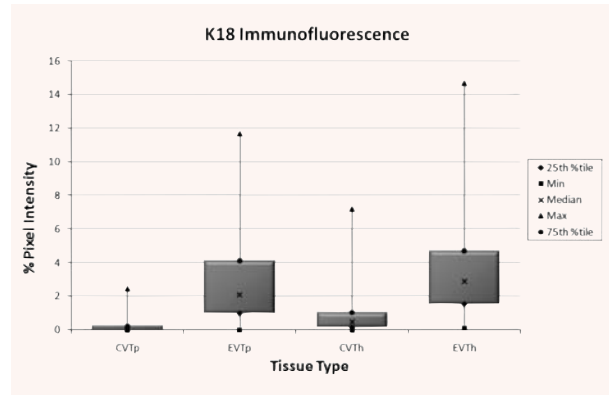


Fig. 6 Boxplot showing interquartile range of the CLSM immunofluorescence data using the anti-keratin-18 antibody on pre-eclamptic chorionic villous trophoblast (CVTp) and extravillous trophoblast (EVTp) and healthy chorionic villous trophoblast (CVTh) and extravillous trophoblast (EVTh). The minimum median and maximum values are indicated by the key and the whisker shows the range.

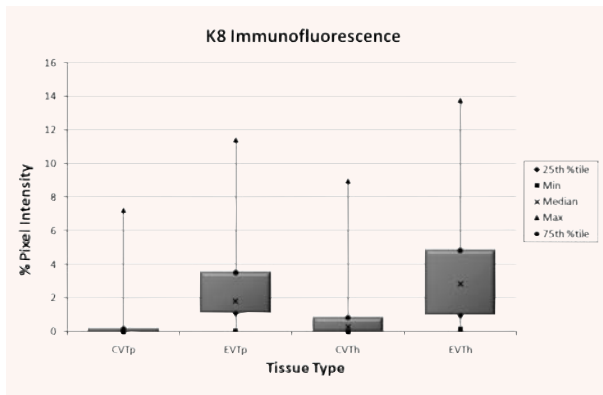


Fig. 5 Boxplot showing interquartile range of the CLSM immunofluorescence data using the anti-keratin-8 antibody on pre-eclamptic chorionic villous trophoblast (CVTp) and extravillous trophoblast (EVTp), also healthy chorionic villous trophoblast (CVTh) and extravillous trophoblast (EVTh). The minimum median and maximum values are indicated by the key and the whisker shows the range.

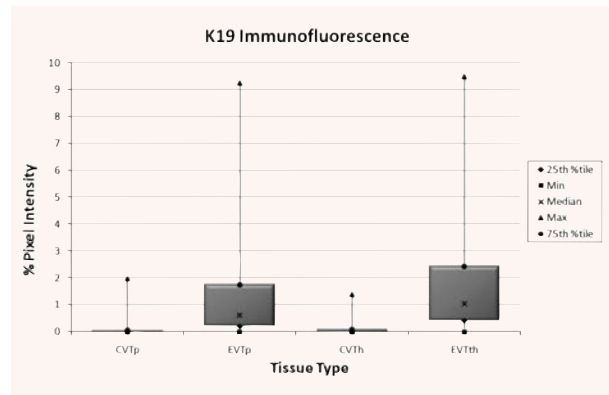


Fig. 7 Boxplot showing interquartile range of the CLSM immunofluorescence data using the anti-keratin-19 antibody on pre-eclamptic chorionic villous trophoblast (CVTp) and extravillous trophoblast (EVTp) and healthy chorionic villous trophoblast (CVTh) and extravillous trophoblast (EVTh). The minimum median and maximum values are indicated by the key and the whisker shows the range.

other cytoplasmic inclusions and cells of mesodermal origin (Fig. 8). Significant reductions in labelling with gold for K7 and K18 were noted in both chorionic villous and extravillous trophoblast from pre-eclamptic placentae (Tables 7 and 8). The counting of gold particles over different areas of tissue allows a quantitation of the amount of keratin in the respective tissues. These immuno-gold counts reflect the results obtained by CLSM pixel intensity data immunofluorescence (See Fig. 4, Table 2 for K7 and Fig. 6, Table 4 for K18) and support them as the techniques are independent.

Discussion

Previous experiments using anti-pan-cytokeratin antibodies had shown an up-regulation of pankeratin in extravillous trophoblast as compared with villous trophoblast [5]. Here, we identify the specific molecular species of keratins that are involved (Table 6); (Figs 2 and 3). The morphological differentiation pathways from the cytotrophoblast stem cell to villous syncytiotrophoblast and extravillous trophoblast are well described in [1] the human placenta, but are not

Table 6 Overview of keratins expression

Keratins (K)	CVT	EVT	Amniotic epithelium
1	–	–	–
2	–	–	–
3	–	–	–
4	–	–	+
5	+	++	+
6	–	–	+
7	+	++	–
8	+	++	+
9	–	–	–
10	–	–	+
12	–	–	–
13	–	–	+
14	–	–	+
15	–	–	–
16	–	–	–
17	–	–	+
18	+	++	+
19	+	++	+
20	–	–	–

The table shows the distribution of 19 distinct molecular forms of keratin (K) in human term extra-embryonic membrane ectoderm including the amniotic epithelium, chorionic villous trophoblast (CVT) and extravillous trophoblast (EVT).

Expression is defined as follows:

(–) = not expressed above background.

(+) = expressed.

(++) = up-regulated.

understood in genetic or physiological terms. Pan-cytokeratin up-regulation of the pathway to extravillous trophoblast was described by our group previously. Here we have shown a statistically significant increase in the percentage median pixel intensity of K7, 8, 18 and 19 immunofluorescence from the villous trophoblast to the extravillous trophoblast. In addition, an observed up-regulation of K5 was detected (see Fig. 1H).

There is also a down-regulation in pre-eclamptic villous and extravillous trophoblast anti-pan-cytokeratin immunofluorescence

with respect to their healthy control tissues (Tables 2–5); (Figs 4–7) [4, 5]. Differences in the expression of keratin in human extraembryonic membranes at term in this study confirm earlier work of Muhlhauser *et al.* [22] with K13, which is expressed only on the amniotic epithelium. We found a lack of expression of K4 and K16 amongst others in the basal plate specifically in this study.

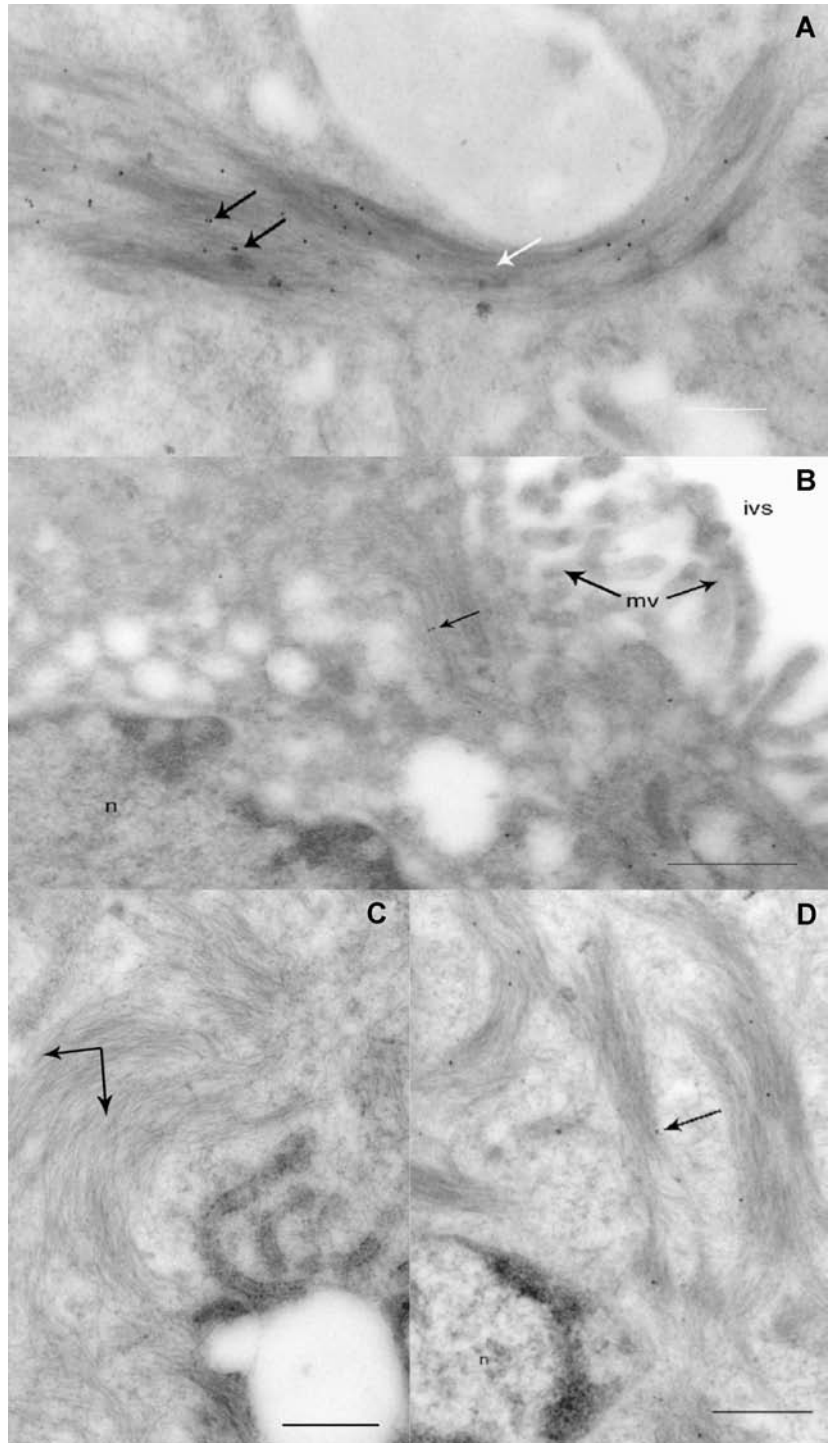
The functions of extravillous trophoblast cells are not fully defined although they are clearly a distinct differentiation state different from villus trophoblast. The fact that EVT do not form an even and complete layer renders a conventional epithelial function such as separation of two compartments or inter-compartment transport most unlikely. This is the general case despite our observation of possibly atavistic alignment of small sequences of cells (Fig. 1E). The possibility that EVTs mediate invasion, attachment, modification of spiral arterioles [26] or signalling to promote the beneficial materno-foetal interaction becomes more likely. The purpose of raised keratin content in EVT beyond that found in chorionic villous trophoblast remains enigmatic. Fluid impermeabilisation ('waterproofing'), reinforcement of basal plate mechanical integrity, a platform for polarized extracellular matrix secretion are reasonable conjectural functions. Whatever the actual function(s), it appears it/they persist until parturition.

The anti-keratin immunofluorescence difference between healthy and pre-eclamptic chorionic villous trophoblast was statistically significant in all 4 keratins (K7, 8, 18 and 19). The differences observed between healthy and pre-eclamptic extravillous trophoblast did not reach significance at the confocal microscopy level but were statistically significant when electron microscopy was employed for anti-keratins 7 and 18 immuno-gold labelling despite the smaller sample areas used by this method and the fact that samples from only 4 placentae were studied (Tables 7 and 8); (Figs 8–10). It is hard to understand the reason for this and we should be cautious in our interpretation. The labelling whilst technically difficult to achieve and of low efficiency was highly selective and the background counts were low and this may have been important. The significant down-regulation of CVT keratins in pre-eclampsia may contribute to one of the mechanisms proposed to underlie this condition, namely that the increased deportation of trophoblast micro-particles into the maternal circulation causes an increased vascular inflammatory reaction. We suggest that the trophoblast in pre-eclamptic placentae might be cytoskeletally weaker and therefore tend to be deported in greater quantity. The selective weakening of the population of trophoblast in contact with maternal blood (the chorionic villous trophoblast) as opposed to the populations in contact with maternal decidua is an observation that is consistent with this hypothesis.

An interesting extension of this study would be to examine the keratin content of deported trophoblast emboli to establish whether these structures better reflect the keratin content of villous trophoblast than extravillous trophoblast emboli. Indeed it is even possible that keratin-related immunofluorescence could be less than in villous trophoblast.

One other point worth raising is that the maternal systemic effects of pre-eclampsia, which appear to be expressed through

Fig. 8 (A) Transmission electron micrograph of intermediate filament bundles associated with anti-K18 coated 10-nm colloidal gold particles. Gold particles (black arrows) are seen over the filament bundle (white arrow) but not the surrounding cytoplasm. (B) In this transmission electron micrograph of chorionic villous trophoblast relatively few keratin fibres are seen and there are correspondingly less anti-K18 conjugated gold particles (arrow). Note that areas such as the nucleus (n), microvilli (mv) and intervillous space (ivs) are entirely unlabelled with gold particles. (C) Keratin filaments without gold particles are observed in this negative control section of extravillous trophoblast exposed to colloidal gold in the absence of first step antibody to keratin 18. (D) Intermediate filaments associated with anti keratin 7 conjugated 10-nm colloidal gold particles (arrow) became detectable only after epitope unmasking. Note that the nucleus and non-intermediate filament containing cytoplasm are unlabelled.



endothelium [27], are reduced upon delivery of the placenta. The presence of hydatidiform molar tissue is an additional risk factor [25]. This raises the possibility that the potential hypertensive toxicity of deported trophoblast is enhanced by genes expressed

in the placenta, which have been epigenetically imprinted in the androgenetic line. This may give a clue as to which of the phenotypically expressed components of chorionic villi are mediators of the condition as only a subset of genes is imprinted.

Table 7 Descriptive statistics of K7 immunogold labelling

	Observations	Mean	Std. Err	Std. Dev.	95%	CI
CVTh	23	1.578	0.1562	0.7490	1.2542	1.9019
CVTp	14	0.926	0.0748	0.2800	0.7643	1.0877
EVTh	30	3.700	0.2341	1.2820	3.2213	4.1787
EVTp	21	1.545	0.29852	1.3680	1.92469	2.1677

Independent two sample t-test comparing CVTh and CVTp ($t = 3.7649$, $P < 0.0007$).
Comparing EVTh and EVTp ($t = 5.6809$, $P < 0.0001$).

Table 8 Descriptive statistics of K18 immunogold labelling

	Observations	Mean	Std. Err	Std. Dev.	95%	CI
CVTh	11	2.289	0.3488	1.1570	1.5117	3.0663
CVTp	14	0.912	0.1024	0.3830	0.6909	1.1331
EVTh	14	6.301	0.8504	3.1820	4.4638	8.1382
EVTp	19	2.505	0.2762	1.2040	1.9247	3.0853

Independent two sample t-test comparing CVTh and CVTp ($t = 3.7876$, $P < 0.0026$).
Comparing EVTh and EVTp ($t = 4.2453$, $P < 0.0006$).

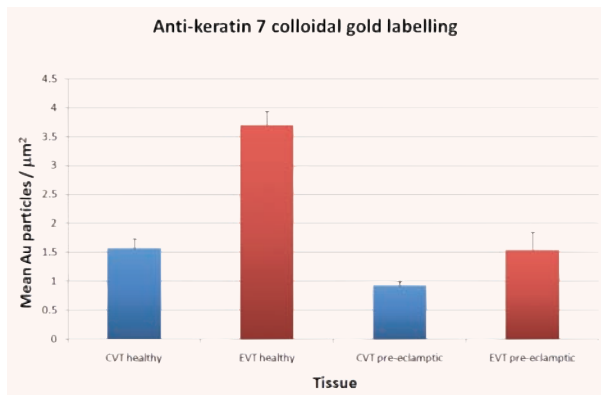


Fig. 9 This bar chart indicates the relatively greater immunoreactivity of the extravillous trophoblast with anti keratin 7 as compared with the chorionic villous trophoblast. There is a reduction of immunoreactivity in both tissues when the pregnancy is pre-eclamptic.

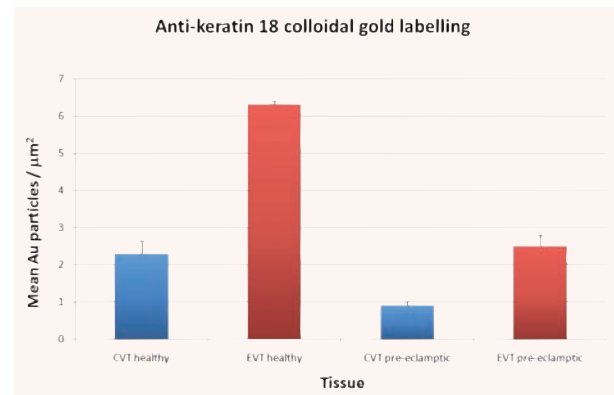


Fig. 10 This bar chart indicates the relatively greater immunoreactivity of the extravillous trophoblast with anti keratin 18 as compared with the chorionic villous trophoblast. There is a reduction of immunoreactivity in both tissues when the pregnancy is pre-eclamptic.

The role of keratin in the process of syncytial morphogenesis has been described previously [6]. Keratin is concentrated for the most part in the apical syncytial cytoplasm and with a less concentrated band associated with the basal surface a pattern reflected in the distribution of dry mass in the syncytiotrophoblast [28, 29].

One of the processes occurring in the apical syncytium is the formation of knots where groups of heterochromatic nuclei become close-packed and form raised features in the syncytial apical surface. This process is held to be the physical manifestation of local apoptosis, which proceeds throughout pregnancy

[30–34]. If this is the case then the down-regulation of keratin may be part of the apoptotic programme. Intermediate filament proteins have been shown to activate classical complement pathways and keratin 1 has been shown to activate the lectin complement pathway [35]. On the basis of this work, there may be a connection between these structures, oxidative stress and innate immune systems that might be relevant to the pathology of pre-eclampsia and pregnancy hypertension.

In conclusion, we have increased the depth of our analysis of keratins to the single molecule level and have shown that the effects previously detected using anti-pan-cytokeratin antibody are reflected in the patterned expression of several but not all

keratins tested. It is amongst the four molecules within chorionic villi that the overall changes in the levels of keratins that correlate with pre-eclamptic pregnancy are to be found.

Acknowledgements

CO is a member of the EMBIC consortium funded under EU Project No. 512040. We thank David Dinsdale for the loan of equipment. JA and BH thank the Ghana government for research scholarships. We thank Chris d'Lacey for his technical assistance and Philip John Morgan for image rendering.

References

1. **Boyd JD, Hamilton WJ.** The Human Placenta. Trinity st., Cambridge W. Heffer and Sons; 1970.
2. **Burton GJ, Hempstock J, Jauniaux E.** Nutrition of the human fetus during the first trimester—a review. *Placenta*. 2001; 22: S70–7.
3. **Mayhew TM, Burton GJ.** Stereology and its impact on our understanding of human placental functional morphology. *Microsc Res Tech*. 1997; 38: 195–205.
4. **Smith RK, Ockleford CD, Byrne S, Bosio P, Sanders R.** Healthy and pre-eclamptic placental basal plate lining cells: quantitative comparisons based on confocal laser scanning microscopy. *Microsc Res Tech*. 2004; 64: 54–62.
5. **Ockleford CD, Smith RK, Byrne S, Sanders R, Bosio P.** Confocal laser scanning microscope study of cytokeratin immunofluorescence differences between villous and extravillous trophoblast: cytokeratin downregulation in pre-eclampsia. *Microsc Res Tech*. 2004; 64: 43–53.
6. **Ockleford CD, Wakely J, Badley RA.** Morphogenesis of human placental chorionic villi: cytoskeletal, syncytioskeletal and extracellular matrix proteins. *Proc R Soc Lond B Biol Sci*. 1981; 212: 305–16.
7. **Ockleford CD, Bradbury FM, Indans I.** Localisation of cytoskeletal proteins in chorionic villi. In: Cedard L, Alsat E, Challier J-C, Chaouat G, Malassine A, editors. Placental communications: biochemical, morphological and cellular aspects. Paris: Colloque INSERM/John Libbey Eurotext Ltd.; 1990. pp. 239–50.
8. **Ockleford CD, Dearden L, Badley RA.** Syncytioskeletons in choriocarcinoma in culture. *J Cell Sci*. 1984; 66: 1–20.
9. **Schweizer J, Bowden PE, Coulombe PA, Langbein L, Lane E, Magin T, Maltais L, Omary M, Parry D, Rogers M, Wright M.** New consensus nomenclature for mammalian keratins. *J Cell Biol*. 2006; 174: 169–74.
10. **Moll R, Franke WW, Schiller DL, Geiger B, Krepler R.** The catalog of human cytokeratins: patterns of expression in normal epithelia, tumors and cultured cells. *Cell*. 1982; 31: 11–24.
11. **O'Guin W, Schermer A, Lynch M, Sun T-T.** Differentiation-specific expression of keratin pairs. In: Goldman RD, Steinert PM, editors. Cellular and molecular biology of intermediate filaments. New York: Plenum Publishing; 1990. pp. 301–34.
12. **Hesse M, Magin TM, Weber K.** Genes for intermediate filament proteins and the draft sequence of the human genome: novel keratin genes and a surprisingly high number of pseudogenes related to keratin genes 8 and 18. *J Cell Sci*. 2001; 114: 2569–75.
13. **Hesse M, Zimek A, Weber K, Magin TM.** Comprehensive analysis of keratin gene clusters in humans and rodents. *Eur J Cell Biol*. 2004; 83: 19–26.
14. **Rogers MA, Winter H, Langbein L, Bleiler R, Schweizer J.** The human type I keratin gene family: characterization of new hair follicle specific members and evaluation of the chromosome 17q21.2 gene domain. *Differentiation*. 2004; 72: 527–40.
15. **Rogers MA, Edler L, Winter H, Langbein L, Beckmann I, Schweizer J.** Characterization of new members of the human type II keratin gene family and a general evaluation of the keratin gene domain on chromosome 12q13.13. *J Invest Dermatol*. 2005; 124: 536–44.
16. **Irvine AD, McLean WH.** Human keratin diseases: the increasing spectrum of disease and subtlety of the phenotype-genotype correlation. *Br J Dermatol*. 1999; 140: 815–28.
17. **Daya D, Sabet L.** The use of cytokeratin as a sensitive and reliable marker for trophoblastic tissue. *Am J Clin Pathol*. 1991; 95: 137–41.
18. **Aplin JD, Haigh T, Jones CJ, Church HJ, Vicovac L.** Development of cytotrophoblast columns from explanted first-trimester human placental villi: role of fibronectin and integrin alpha5beta1. *Biol Reprod*. 1999; 60: 828–38.
19. **Ockleford C, Malak T, Hubbard A, Bracken K, Burton K, Bright N, Blakey G, Goodliffe J, Garrod D, de Lacey C.** Confocal and conventional immunofluorescence and ultrastructural localisation of intracellular strength-giving components of human amniochorion. *J Anat*. 1993; 183: 483–505.
20. **Feng Q, Liu Y, Liu K, Byrne S, Liu G, Wang X, Li Z, Ockleford CD.** Expression of urokinase, plasminogen activator inhibitors and urokinase receptor in pregnant rhesus monkey uterus during early placentation. *Placenta*. 2000; 21: 184–93.
21. **Feng Q, Liu K, Liu YX, Byrne S, Ockleford CD.** Plasminogen activators and inhibitors are transcribed during early macaque implantation. *Placenta*. 2001; 22: 186–99.
22. **Muhlhauser J, Crescimanno C, Kasper M, Zaccheo D, Castellucci M.** Differentiation of human trophoblast populations involves alterations in cytokeratin patterns. *J Histochem Cytochem*. 1995; 43: 579–89.
23. **Fuchs E, Weber K.** Intermediate filaments: structure, dynamics, function, and disease. *Annu Rev Biochem*. 1994; 63: 345–82.
24. **Redman CW, Sargent IL.** Placental debris, oxidative stress and pre-eclampsia. *Placenta*. 2000; 21: 597–602.

25. **ACOG practice bulletin.** Diagnosis and management of preeclampsia and eclampsia. Number 33, January 2002. American College of Obstetricians and Gynecologists. *Int J Gynaecol Obstet.* 2002; 77: 67–75.
26. **Pijnenborg R, Vercruyse L, Hanssens M.** The uterine spiral arteries in human pregnancy: facts and controversies. *Placenta.* 2006; 27: 939–58.
27. **Robb AO, Mills NL, Newby DE, Denison FC.** Endothelial progenitor cells in pregnancy. *Reproduction.* 2007; 133: 1–9.
28. **Ockleford CD.** A quantitative interference light microscope study of human first trimester chorionic villi. *J Microsc.* 1990; 157: 225–37.
29. **Bradbury FM, Ockleford CD.** A confocal and conventional epifluorescence microscope study of the intermediate filaments in chorionic villi. *J Anat.* 1990; 169: 173–87.
30. **Smith SC, Baker PN, Symonds EM.** Placental apoptosis in normal human pregnancy. *Am J Obstet Gynecol.* 1997; 177: 57–65.
31. **Goswami D, Tannetta DS, Magee LA, Fuchisawa A, Redman CWG, Sargent IL, Von Dadelszen P.** Excess syncytiotrophoblast microparticle shedding is a feature of early-onset pre-eclampsia, but not normotensive intrauterine growth restriction. *Placenta.* 2006; 27: 56–61.
32. **Johansen M, Redman CWG, Wilkins T, Sargent IL.** Trophoblast deportation in human pregnancy: its relevance for pre-eclampsia. *Placenta.* 1999; 20: 531–9.
33. **Knight M, Redman CWG, Linton EA, Sargent IL.** Shedding of syncytiotrophoblast microvilli into the maternal circulation in pre-eclamptic pregnancies. *Br J Obstet Gynaecol.* 1998; 105: 632–40.
34. **Sargent IL, Germain SJ, Sacks GP, Kumar S, Redman CWG.** Trophoblast deportation and the maternal inflammatory response in pre-eclampsia. *J Reprod Immunol.* 2003; 59: 153–60.
35. **Collard CD, Montalto MC, Reenstra WR, Buras JA, Stahl GL.** Endothelial oxidative stress activates the lectin complement pathway: role of cytokeratin 1. *Am J Pathol.* 2001; 159: 1045–54.